

Experimental studies of the $\Lambda(1405)$

physics654 – Seminar on exotic multi-quark states

JAKOB KRAUSE

✉ krause@hiskp.uni-bonn.de |  krausejm

Tutor: GEORG SCHELUCHIN

✉ scheluchin@physik.uni-bonn.de

18.06.2021

What is special about the $\Lambda(1405)$?

- ▶ ~~its~~ mass does not fit well into constituent quark models ~~which do predict baryon masses well for other baryons~~
- ▶ invariant mass distribution (line shape) differs significantly from usual BREIT-WIGNER shapes ✓
- ▶ candidate for an exotic multiquark state (bound system of $\bar{K}N$) since its mass lies just below threshold

production

There are ~~(very)~~ many different theoretical approaches to explain this behavior

→ There is need for more experimental data!

~~some plots/pictures?~~

Table of contents

7

Motivation

1. Experimental setup
2. Line-shape measurement
3. Spin-parity measurement
4. Conclusion

1. Experimental setup
2. Line-shape measurement
3. Spin-parity measurement
4. Conclusion

Continuous Electron Beam Accelerator Facility (CEBAF)

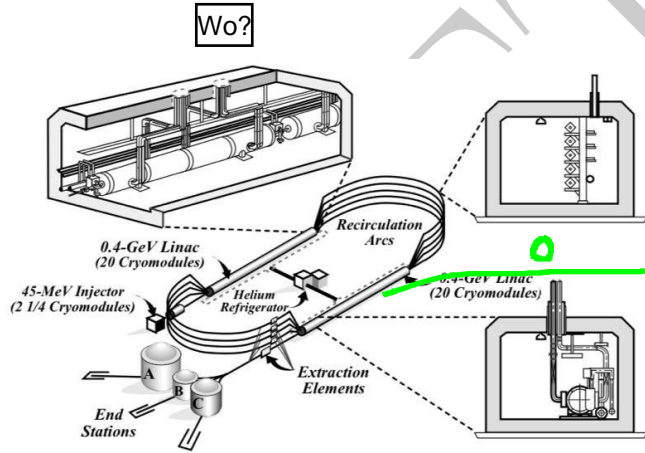


Figure 1: CEBAF layout at Jefferson Lab, [Mecking et al. 2003]

Das wird nicht in beamer gemacht(kein sin für referenzen)

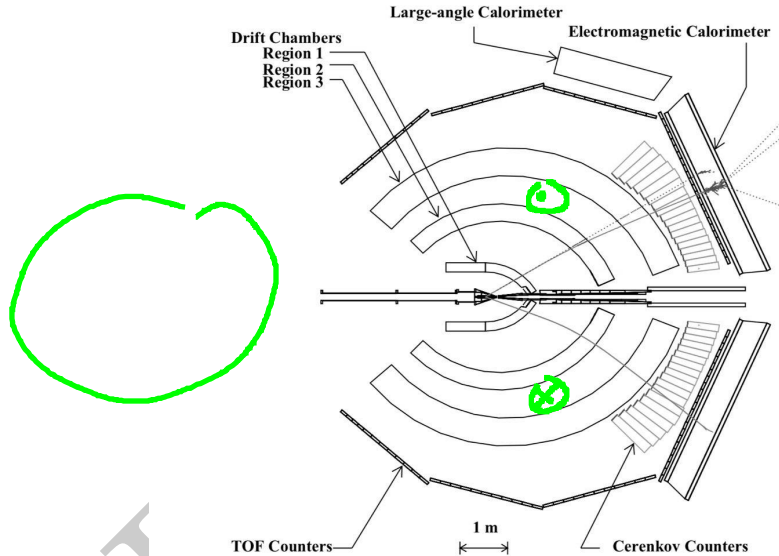
Continuous Electron Beam Accelerator Facility (CEBAF)

How can we access $\Lambda(1405)$ with this setup?

- ▶ employ radiator target for the electrons
- ▶ generate high energy photons using the *bremsstrahlung* process
- ▶ shoot high energy photons on proton target (LH2)
- ▶ then we can observe $\gamma p \rightarrow K^+ \Lambda(1405)$ while knowing p_γ, p_p

~~Wiso zeigst du den Tagger nicht stattdessen?~~

CEBAF Large Acceptance Spectrometer (CLAS)



Magnetfeld \perp

~~Figure 2:~~ CLAS layout at Jefferson Lab, [Mecking et al. 2003]

1. Experimental setup
2. Line-shape measurement
3. Spin-parity measurement
4. Conclusion

Reaction kinematics

Reaction	Strong Final State	Undetected	Particles X
		$K^+ p \pi^-(X)$	$K^+ \pi^+ \pi^-(X)$
$\gamma + p \rightarrow K^{*+} \begin{cases} \Lambda(1405) \\ \Lambda(1520) \end{cases}$	~33%	$\Sigma^+ \pi^-$	π^0 (52%) n (48%)
	~33%	$\Sigma^0 \pi^0$	$\pi^0 \gamma$ (64%)
	~33%	$\Sigma^- \pi^+$	n (100%)
	6%	$K^+ \Lambda \pi^0$	
	6%		
$\gamma + p \rightarrow K^+ + \Sigma^0(1385)$	87%	π^0 (64%)	
$\gamma + p \rightarrow K^{*+} + \Sigma^0$		$\pi^0 \gamma$ (64%)	
$\gamma + p \rightarrow K^{*0} + \Sigma^+$		π^0 (52%)	n (48%)

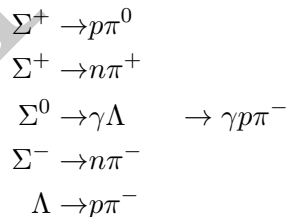


Figure 3: Possible and studied reactions in the analysis of the lineshapes of $\Lambda(1405)$, taken from [Moriya, Schumacher, Adhikari et al. 2013]

Event selection

There are two sets of reactions that the detector sees

1. $K^+ p \pi^-$ ✗
2. $K^+ \pi^+ \pi^-$ ✗

There are many cuts that can be made that apply to both

Initial selection of particles

▶ ~~Initial~~ final state Kaon selection

▶ fiducial cuts

▶ remove false K^+ due to π^+ or p

▶ Loose ΔTOF cut ($\Delta\text{TOF} = t_{\text{meas}} - t_{\text{calc}} = t_{\text{meas}} - \frac{l\sqrt{p^2 + m_0^2}}{cp}$)

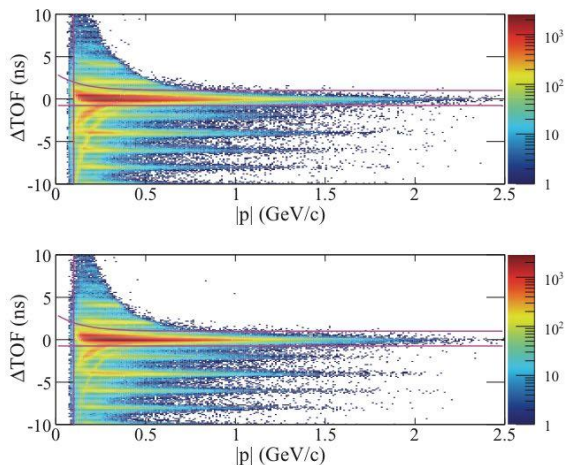
▶ vertex z cut

▶ minimum $|\mathbf{p}|$ cuts

▶ Precise ΔTOF cuts

- p, beta particle identification

Event selection



~~Figure 4:~~ ΔTOF for π^\pm @ $2.35 < W < 2.45$ GeV, applied cuts are shown in magenta. [Moriya, Schumacher, Adhikari et al. 2013]

Beide sehen ziemlich gleich aus ich würde nur eins z

Event selection

Data divided into bins of 100 MeV \sqrt{s} and 0.1 $\cos(\theta_{K^+}^{\text{CMS}})$

~~In all channels, the data was divided into 10 bins of energy spanning 100 MeV in the CMS energy $W = \sqrt{s}$ and 20 angle bins in the CMS kaon angle.~~

→ the following analysis was performed independently in every bin of energy and angle!

Event selection

extracting $\Lambda\pi^0$ and $\Sigma^+\pi^-$

- reminder: $\Lambda \rightarrow p\pi^-, \Sigma^+ \rightarrow p\pi^0$
- final state particles: $K^+p\pi^-(\pi^0)$
- determine p_π via missing mass fit
- apply cuts based on fits to the invariant masses $M_{p\pi^-}$ and $M_{p\pi^0}$

extracting $\Sigma^+\pi^-$ and $\Sigma^-\pi^+$

- reminder: $\Sigma^\pm \rightarrow n\pi^\pm$
- final state particles: $K^+\pi^+\pi^-(n)$
- determine p_n via missing mass fit
- apply cuts based on fits to the invariant masses $M_{n\pi^\pm}$

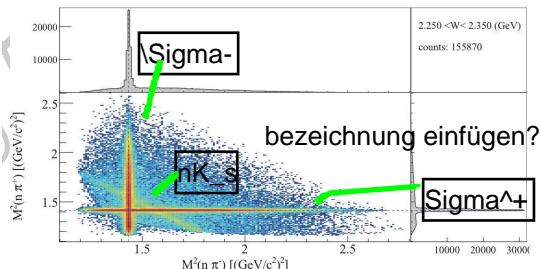
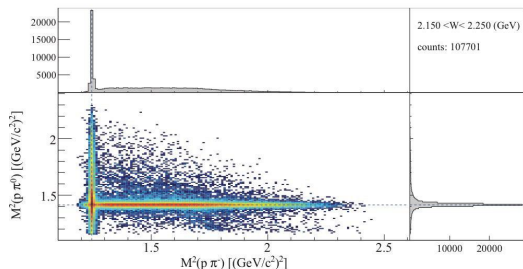


Figure 5: DALITZ-like plots of the above mentioned invariant masses, taken from [Moriya, Schumacher, Adhikari et al. 2013]

Event selection

extracting $\Sigma^0\pi^0$

- reminder: $\Sigma^0 \rightarrow \gamma\Lambda \rightarrow \gamma p\pi^-$
- final state particles: $K^+p\pi^- (\gamma\pi^0)$ - missing mass fit is not applicable here: demand the missing mass is sufficiently greater than m_π
- make cuts based on the invariant mass $M_{p\pi^-}$
- now the missing mass ($\gamma p \rightarrow K^+ X$) gives the $\Sigma^0\pi^0$ lineshape

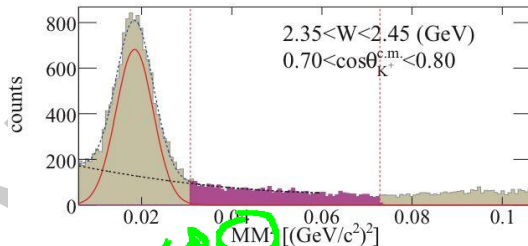


Figure 6: Invariant mass of the $\gamma\pi$ system, selection range in magenta. Taken from [Moriya, Schumacher, Adhikari et al. 2013]

Measurements and analysis

- ▶ Now the signal regions have been established
- ▶ The true lineshape of the $\Lambda(1405)$ has to be extracted from the vast of reactions
→ any other contributions have to be ~~excluded~~ **subtracted**
- ▶ Strategy: use of MONTE-CARLO fits to the data, simulating the contribution of other resonances using the PDG widths and masses

~~I will not really go into detail here...(??)~~

Measurements and analysis

Some fit results:

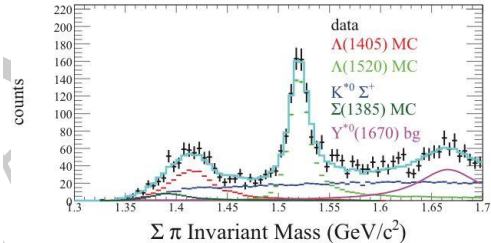
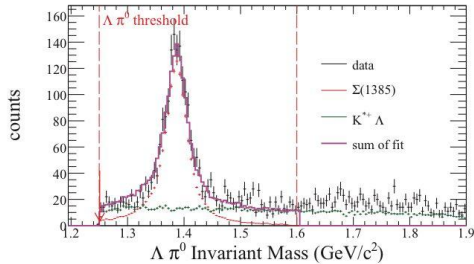


Figure 7: Sample fit results of invariant mass spectra for a single bin in energy and angle, taken from [Moriya, Schumacher, Adhikari et al. 2013]

Interpretation of the results

Having subtracted all unwanted reactions, one can obtain the true $\Lambda(1405)$ lineshapes:

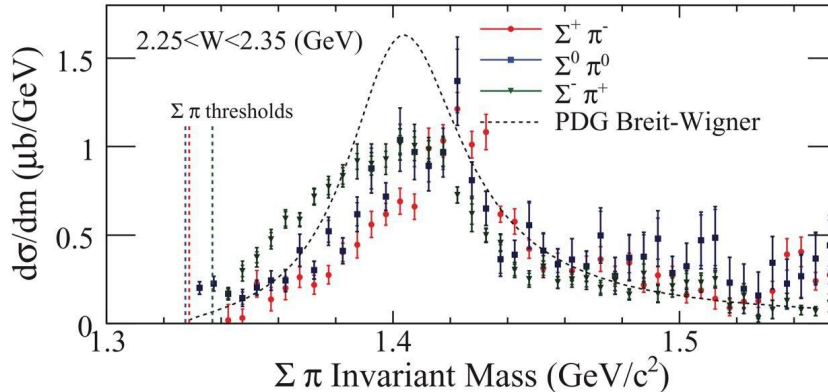
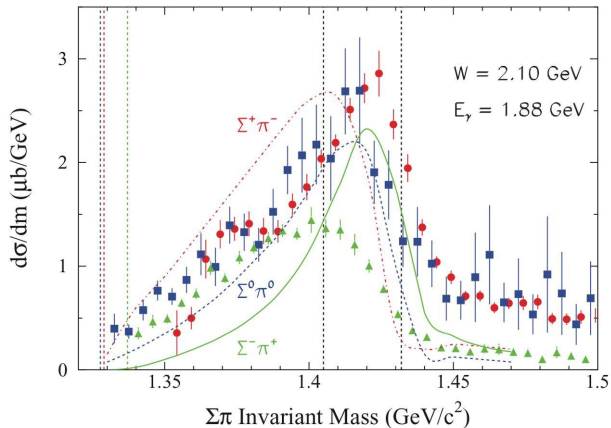


Figure 8. Lineshapes of the $\Lambda(1405)$ for the 3 different decay channels and the PDG BREIT-WIGNER. The data were summed over all angles for better statistics. [Moriya, Schumacher, Adhikari et al. 2013]

Interpretation of the results

There are in fact predictions of the lineshapes differing by decay channel [Nacher et al. 1999].

→ main idea: not one amplitude, but two due to isospin decomposition.



~~Figure 9:~~ Lineshapes of the $\Lambda(1405)$ for the 3 different decay channels and the prediction of [Nacher et al. 1999], ~~taken from~~ [Moriya, Schumacher, Adhikari et al. 2013]

Interpretation of the results

MORIYA ET AL. saw two main reasons for the lineshapes differing from a simple BREIT-WIGNER:

1. Isospin decomposition
2. channel coupling between the detected $\Sigma\pi$ and $N\bar{K}$ final states

Isospin decomposition

let

$$|t_I|^2 = |\langle I, 0 | T^{(I)} | \gamma p \rangle|^2,$$

then we can write (neglecting $I = 2$ using CGK)

$$|T_{\pi^-\Sigma^+}|^2 = \frac{1}{3}|t_0|^2 + \frac{1}{2}|t_1|^2 - \frac{2}{\sqrt{6}} \cos \phi_{01}$$

$$|T_{\pi^0\Sigma^0}|^2 = \frac{1}{3}|t_0|^2$$

$$|T_{\pi^+\Sigma^-}|^2 = \frac{1}{3}|t_0|^2 + \frac{1}{2}|t_1|^2 + \frac{2}{\sqrt{6}} \cos \phi_{01}$$

Channel coupling

the t_I are described by one or two BREIT-WIGNER amplitudes with mass dependent widths Γ

→ modify the amplitude preserving analyticity [Flatté 1976] including the $N\bar{K}$ decay channel available at threshold $m_K + m_p \approx 1434 \text{ MeV}$

Interpretation of results

Fits with two $I = 1$ and one $I = 0$ amplitudes lead to best agreement with measured data also show $\Sigma^-\pi^+, \Sigma^0\pi^0$?

ja zeig ein drittel von allen

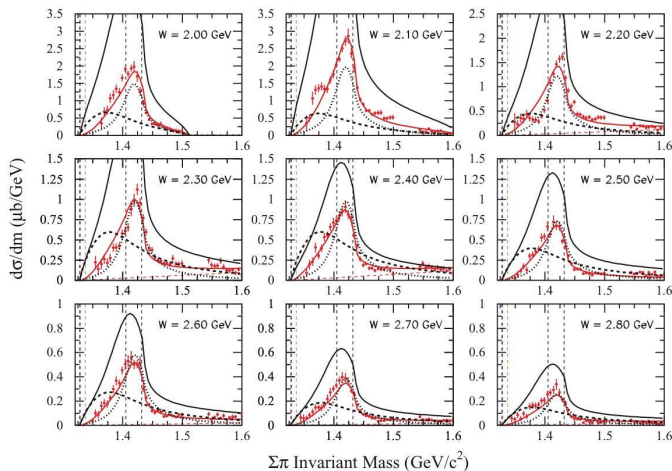


Figure 10: Data and fits for $\Sigma^+\pi^-$ for different bins in W . $I = 0$ (solid black), narrow $I = 1$ (dotted black) and wide $I = 1$ (dashed black). Background in dashed red. [Moriya, Schumacher, Adhikari et al. 2013]

1. Experimental setup
2. Line-shape measurement
3. Spin-parity measurement
4. Conclusion

Theoretical basics Spin

The $\Lambda(1405)$ is so far (mostly) assumed to have $J^P = \frac{1}{2}^-$, but this has not been determined experimentally

Measuring spin

- ▶ consider the strong decay $Y^* \rightarrow Y\pi$, with J^P the spin and parity of Y^*
- ▶ the $Y\pi$ angular distribution will only depend on J

$$I(\theta_Y) = \text{const.} \qquad J = 1/2$$

$$I(\theta_Y) \propto 1 + \frac{3(1-2p)}{2p+1} \cos^2 \theta_Y \qquad J = 3/2,$$

where θ_Y is the polar angle of the decay direction of Y in the Y^* rest frame, p describes the fraction of spin projections along the z axis

- ▶ uniform decay pattern is best evidence for spin $J = 1/2$

[Moriya, Schumacher, Aghasyan et al. 2014]

Measuring parity

- ▶ the key to accessing the parity lies in determining the Polarization transfer to the decay product Y which we will denote \mathbf{Q}
- ▶ the angular distribution of \mathbf{Q} will only depend on \mathbf{P}

$$\mathbf{Q}(\theta_Y) = \text{const.} \quad J^P = 1/2^-$$

$$\mathbf{Q}(\theta_Y) = -\mathbf{P} + 2(\mathbf{P} \cdot \mathbf{q})\mathbf{q} \quad J^P = 1/2^+$$

- ▶ \mathbf{Q} can be measured from weak decay angular distribution of Y

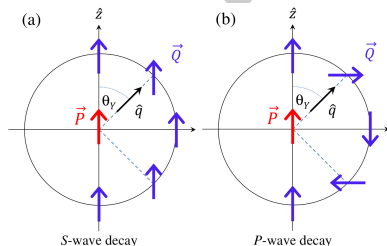


Figure 11: Polarization transfer in the strong decay $Y^* \rightarrow Y\pi$, taken from [Moriya, Schumacher, Aghasyan et al. 2014]

[Moriya, Schumacher, Aghasyan et al. 2014 and Ref. therein]

Event selection

- ▶ select kinematic region where the $\Sigma\pi$ invariant mass is dominated by the $\Lambda(1405) \rightarrow M_{\Sigma\pi} \in 1.30 \text{ GeV to } 1.45 \text{ GeV}$
- ▶ inspect nine bins in energy and angle, namely with CM energy at 2.6, 2.7 and 2.8 GeV and the three forwardmost kaon angle bins each

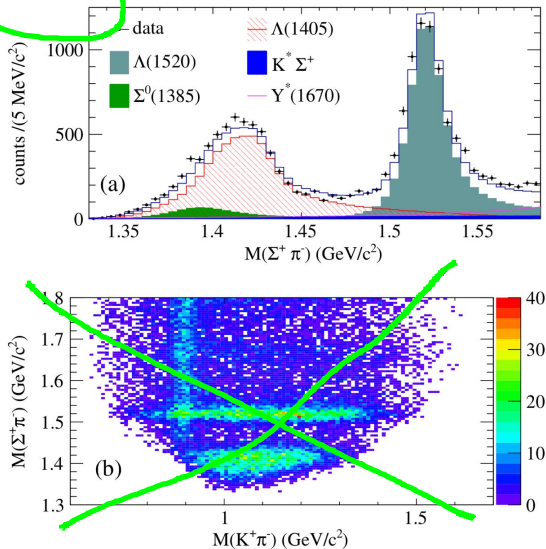


Figure 12: $\Sigma\pi$ and $K\pi$ invariant mass in the vicinity of the $\Lambda(1405)$, taken from [Moriya, Schumacher, Aghasyan et al. 2014]

aufspalten + extra bild

Analysis procedure

- 1 ► plot the angular distribution of the projections $\cos \theta_\Sigma$ and $\cos \theta_p$ for each bin
- 1 ► test each spin hypothesis using MONTE-CARLO maximum likelihood fits, which employ angular decay probability distributions according to each hypothesis for $\Sigma\pi$ and $p\pi$. From the fit Q_z will be determined
- 2 ► test parity hypotheses by determining $Q_z(\cos \theta_\Sigma)$
- 1 ► compare each hypothesis by calculating a χ^2 probability

Result: data is consistent with $J^P = 1/2^-$ but does in principle not rule out $J^P = 3/2^+$. $1/2^+$ and $3/2^-$ can be discarded.

Measurements and analysis

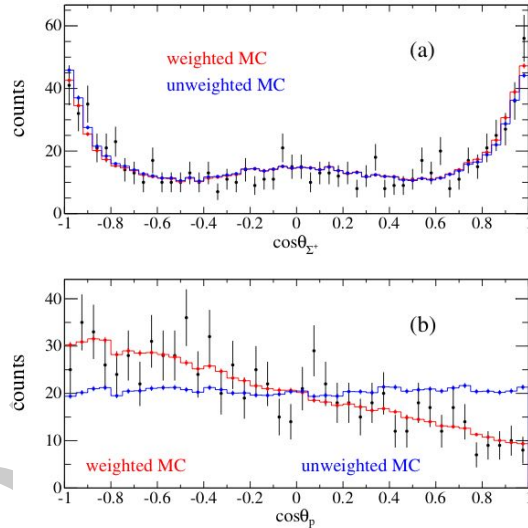


Figure 13: Distributions of the projections of (a) $\cos \theta_{\Sigma^+}$ and (b) $\cos \theta_p$ @ $2.65 < W < 2.75$ GeV and $0.70 < \cos \theta < 0.80$, taken from [Moriya, Schumacher, Aghasyan et al. 2014]

Measurements and analysis

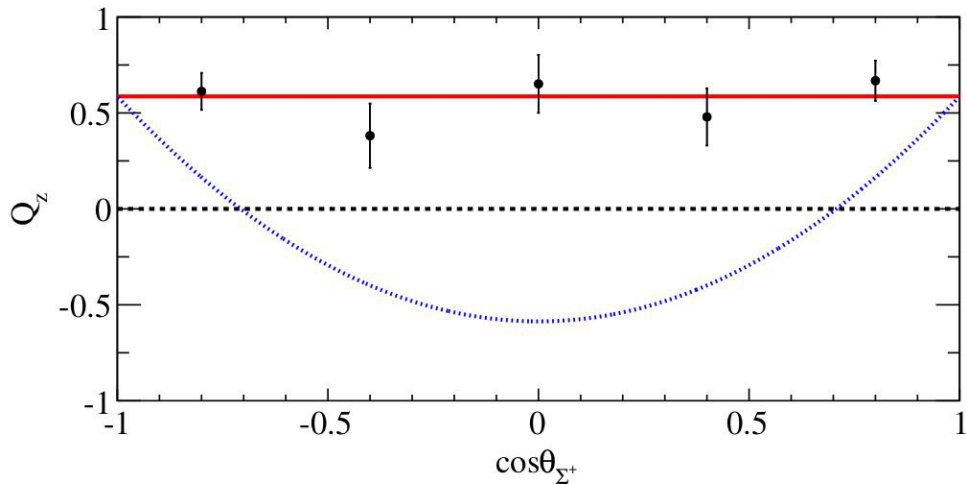


Figure 14: angular distribution of the polarization Q_z @ $2.65 < W < 2.75$ GeV and $0.70 < \cos\theta < 0.80$. Red: average, blue: expectation for P -wave decay. Taken from [Moriya, Schumacher, Aghasyan et al. 2014]

1. Experimental setup
2. Line-shape measurement
3. Spin-parity measurement
4. Conclusion

Conclusion





Lineshape measurement

- ▶ the CLAS detector was used to study $\gamma p \rightarrow K^+ \Lambda(1405)$
- ▶ after selecting the correct events the true lineshape was extracted using MONTE-CARLO sim. of the yield of other resonances
- ▶ the lineshapes in different decay channels differ from each other and from a simple BREIT-WIGNER
- ▶ a phenomenological isospin decomposition model was able to describe the data

Spin parity measurement

- ▶ the angular distribution of the decay $\Lambda(1405) \rightarrow \Sigma^+ \pi^-$ was studied
- ▶ the angular distributions were tested against various J^P hypotheses
- ▶ the data is consistent with $J^P = 1/2^-$ but does not exclude $J^P = 3/2^+$

References

-  Flatté, S.M. (1976). ‘Coupled-channel analysis of the $\pi\eta$ and $K\bar{K}$ systems near $K\bar{K}$ threshold’. In: *Physics Letters B* 63.2, pp. 224–227. ISSN: 0370-2693. DOI: [https://doi.org/10.1016/0370-2693\(76\)90654-7](https://doi.org/10.1016/0370-2693(76)90654-7). URL: <https://www.sciencedirect.com/science/article/pii/0370269376906547>.
-  Mecking, B.A. et al. (2003). ‘The CEBAF large acceptance spectrometer (CLAS)’. In: *Nuclear Instruments and Methods in Physics Research Section A: Accelerators, Spectrometers, Detectors and Associated Equipment* 503.3, pp. 513–553. ISSN: 0168-9002. DOI: [https://doi.org/10.1016/S0168-9002\(03\)01001-5](https://doi.org/10.1016/S0168-9002(03)01001-5). URL: <https://www.sciencedirect.com/science/article/pii/S0168900203010015>.
-  Moriya, K., R. A. Schumacher, K. P. Adhikari et al. (Mar. 2013). ‘Measurement of the $\Sigma\pi$ photoproduction line shapes near the $\Lambda(1405)$ ’. In: *Phys. Rev. C* 87 (3), p. 035206. DOI: 10.1103/PhysRevC.87.035206. URL: <https://link.aps.org/doi/10.1103/PhysRevC.87.035206>.
-  Moriya, K., R. A. Schumacher, M. Aghasyan et al. (Feb. 2014). ‘Spin and parity measurement of the $\Lambda(1405)$ baryon’. In: *Phys. Rev. Lett.* 112 (8), p. 082004. DOI: 10.1103/PhysRevLett.112.082004. URL: <https://link.aps.org/doi/10.1103/PhysRevLett.112.082004>.